

Article

Comparing Mixed-Media and Conventional Slow-Sand Filters for Arsenic Removal from Groundwater

Karolina M. Śmiech¹, Aize Tolsma² , Tímea Kovács^{2,3}, Vlade Dalbosco^{3,4}, Kamuran Yasadi⁵, Leo Groendijk² and Luewton L. F. Agostinho^{1,3,*}

¹ Water Technology Research Group, NHL-Stenden University of Applied Sciences, Rengerslaan 10, 8917 DD Leeuwarden, The Netherlands; karolina.smiech@hvhl.nl

² Van Hall Larenstein University of Applied Sciences, Agora 1, 8934 CJ Leeuwarden, The Netherlands; aize.tolsma@hvhl.nl (A.T.); k.timi1986@gmail.com (T.K.); leo.groendijk@hvhl.nl (L.G.)

³ Centre of Expertise Water Technology, Agora 4, 8934 CJ Leeuwarden, The Netherlands; vlade@dalbosco.net

⁴ Department of Sanitary and Environmental Engineering, Faculty of Engineering, Federal University of Santa Catarina, Campus João David Ferreira Lima, s/n, Trindade, Florianópolis-SC 88040-900, Brazil

⁵ Wageningen University and Research Centre, Droevendaalsesteeg 4, 6708 PB Wageningen, The Netherlands; yasadi@ecm.nl

* Correspondence: luewton.agostinho@hvhl.nl

Received: 13 November 2017; Accepted: 8 January 2018; Published: 29 January 2018

Abstract: Arsenic contamination of groundwater is a major public health concern worldwide. The problem has been reported mainly in southern Asia and, especially, in Bangladesh. Slow-sand filters (SSF) augmented with iron were proven to be a simple, low-cost and decentralized technique for the treatment of arsenic-contaminated sources. In this research, three pilot-scale SSF (flowrate 6 L·h⁻¹) were tested regarding their capability of removing arsenic from groundwater in conditions similar to those found in countries like Bangladesh (70 µg As(III) L⁻¹, 26 °C). From the three, two filters were prepared with mixed media, i.e., sand mixed with corrosive iron matter (CIM filter) and iron-coated sand (ICS filter), and a third conventional SSF was used as a reference. The results obtained showed that the CIM filter could remove arsenic below the World Health Organization (WHO) guideline concentration of 10 µg·L⁻¹, even for inlet concentrations above 150 µg·L⁻¹. After 230 days of continuous operation the arsenic concentration in the effluent started increasing, indicating depletion or saturation of the CIM layer. The effluent arsenic concentration, however, never exceeded the Bangladeshi standard of 50 µg·L⁻¹ throughout the whole duration of the experiments.

Keywords: arsenic; groundwater; slow sand filter; corrosive iron matter; iron-coated sand

1. Introduction

Arsenic contamination of groundwater is a major public health concern in southern Asia, particularly in Bangladesh [1–4]. After 14-year study about the arsenic problem in Bangladesh Chakraborti et al. estimated that about 36 million inhabitants could be drinking water contaminated above the World Health Organization (WHO) guideline of 10 µg·L⁻¹ and about 22 million above the 50 µg·L⁻¹ limit established by the Bangladeshi government [1,5]. In more recent work, the same authors mentioned that from 51,731 investigated hand-made tube-wells, 43% had arsenic concentrations above 10 µg·L⁻¹ and 27% above 50 µg·L⁻¹ [2]. Furthermore, in 7.7% of the investigated wells the arsenic concentration exceeded 300 µg·L⁻¹ and in 0.6% the concentration was higher than 1 mg·L⁻¹ [2].

The problem of drinking water contaminated with arsenic in the country started in the 1980s, when the local government recommended the construction of hand-made tube-wells as an alternative source of drinking water. The intention was to reduce the number of waterborne disease cases caused

by contaminated surface water sources. Tube-wells provided easy access to pathogen-free groundwater. However, extended studies carried out in the 1990s revealed that the groundwater sources contained elevated concentrations of geogenic-origin arsenic [2,6]. Further medical research showed that a vast majority of the Bangladeshi population had symptoms related to long-term exposure to arsenic, such as skin lesions, lung irritation and skin and internal organ cancer [2,7,8].

Arsenic concentration in water can be reduced with the appropriate treatment. Commercially available methods include chemical coagulation–precipitation, ion exchange and membrane separation [9,10]. The main bottlenecks of the above mentioned technologies include relatively high investment costs, energy consumption and their complex maintenance and technical requirements; which makes them (mostly) unsuitable for use at a household level and/or in rural areas. More recently, several “simpler” solutions have been proposed. They comprise, basically, sand filters augmented with various forms of iron for the adsorption and co-precipitation of the arsenic species [11,12]. Examples of such filters are: (i) the SONO filter—based on so called composite iron matter in combination with sand, gravel and charcoal [13]; (ii) the Kanchan arsenic filter (KAF)—a modified slow sand filter with iron nails used for enhanced arsenic removal [14]; (iii) the Two-Kolshi filter—based on co-precipitation and filtration, which uses ferric chloride as a coagulant, calcium hypochlorite as an oxidant/disinfectant, and charcoal powder as an adsorbent [15]; and (iv) the Three-Kolshi filter—filled with iron fillings, sand and wood charcoal [15,16].

In this research, three pilot-scale slow-sand filters (SSF) were compared in terms of their arsenic removal capability: one conventional slow-sand filter (used as reference) and two mixed media (sand and iron) filters. The mixed-media filters were prepared with different types of iron materials mixed into the sand media, namely: corrosive iron matter (CIM filter) and iron-coated sand (ICS filter). To simulate Bangladeshi conditions, the filters were placed in a climate room at 26 °C and fed with arsenic-spiked groundwater at a concentration $\sim 70 \mu\text{g}\cdot\text{L}^{-1}$ i.e., the value measured in groundwater samples received from the Manikganj region of Bangladesh.

The filters were kept in continuous operation for 230 days and monitored regarding their arsenic-removal efficiency and the following parameters: pH, dissolved oxygen (DO), electrical conductivity, redox potential and iron and manganese concentration. Additional microbiological and spectroscopic analysis of the filter media were performed to better understand the arsenic removal mechanism.

The system proposed in our investigation differs from other systems (currently available on the market), e.g., the SONO filter [13], the Kanchan arsenic filter [14] and two- and three-Kolshi filters [15,16], basically due to its composition, configuration and capacity. In practical terms, this system relies solely on the implantation of iron waste products as sorbents in existent sand filters. Thus, it can be considered as a simple upgrade of already existing slow-sand filters. Conversely, the SONO, Kanchan and Three-Kolshi, need to be purchased and installed separately. Furthermore, the other commercial systems mentioned are mostly designed for household usage, while the system presented in this paper can operate at a village or community level.

2. Materials and Methods

Three pilot-scale slow-sand filters containing different filtration media were constructed for this research: Filter 1 (reference filter) containing sand and gravel, Filter 2 (CIM filter) containing sand, gravel and a layer of corrosive iron matter, Filter 3 (ICS filter) containing sand, gravel and a layer of iron-coated sand. The design of the pilot installation is shown in Figure 1.

The filters were made using PVC tubes 150 cm long and 250 mm in diameter. Seven taps were installed in each tube: two at the bottom, for effluent drainage and backwashing, and five on the lateral side, at different heights (10, 20, 50, 70 and 90 cm from the bottom of the filter) along the filtration media to allow sampling at different positions in the filtration column.

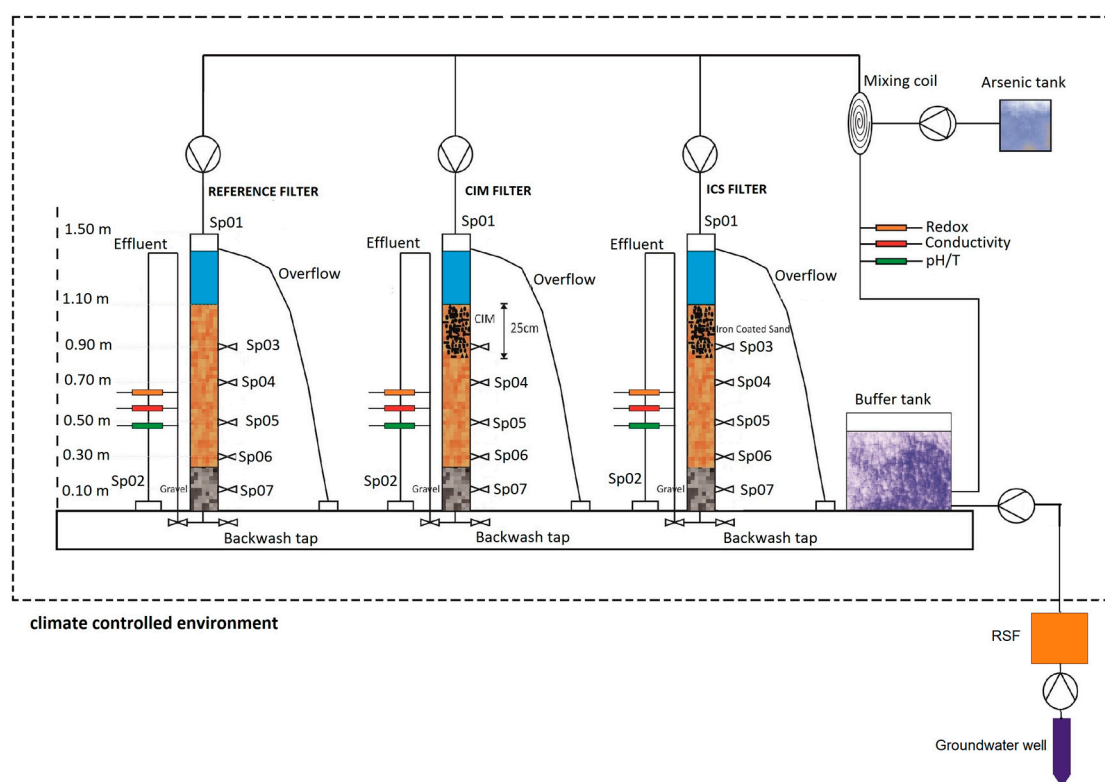


Figure 1. Experimental setup consisting of three pilot-scale slow-sand filters containing different filtration media: sand and gravel (reference filter); sand, gravel and corrosive iron matter (CIM); sand, gravel and iron-coated sand (ICS).

The influent was supplied at the top of each filter with a dedicated peristaltic feed pump (Cole–Parmer-type Masterflex L/S 6-6000, Vernon Hills, IL, USA) at a flow rate of $100 \text{ mL}\cdot\text{min}^{-1}$. To provide a constant inlet concentration of arsenic ($\sim 70 \mu\text{g}\cdot\text{L}^{-1}$), a solution containing concentrated arsenic (III) oxide was dosed to the influent with a magnetic pump (KNF lab type Simdos 10, Trenton, NJ, USA).

The following parameters were measured in-line (influent and effluents) with Endress + Hauser sensors (Reinach, Switzerland): redox potential (sensor type Orbisint CPS11D), electrical conductivity (sensor type Condumax CLS21D), and pH (sensor type Orbisint CPS12D). The measured values were logged by two universal multichannel controllers (Endress + Hauser type CM448). The influent was stored in two buffer tanks (1 m^3), which could provide enough volume for a 72 h continuous supply for the filters. On each working day one of the buffer tanks was emptied and filled again with fresh groundwater. To maintain the temperature of the influent between 24 and 26 °C (the average groundwater temperature in Bangladesh), the entire installation was placed in a 26 °C climate room.

More information about the preparation of the filter media is presented subsequently.

2.1. Common Media (In All Filters)

The bottom of all filters was filled with four 7 cm layers of gravel and coarse sand. The layers were prepared as follows (from top-down): (i) natural moist and calibrated gravel (filter gravel), diameter 16–32 mm; (ii) natural moist and calibrated gravel (filter gravel), diameter 4–16 mm; (iii) dried and calibrated gravel (filter gravel), diameter 2–4 mm; and (iv) dried and calibrated coarse sand (filter sand), diameter 0.7–1 mm. Above the gravel media a 57 cm layer of sand media was placed. The sand was dried and calibrated, with coefficient of uniformity (C_u) of 1.86 and diameter of 0.14–4 mm.

2.2. Specific Media

Filter 1 (reference): On top of the 57 cm sand layer, an extra 25 cm sand layer (same specifications) was placed.

Filter 2 (CIM filter): On top of the 57 cm sand layer, a 25 cm layer containing CIM mixed with sand was placed. The CIM and sand layer was prepared as follows: 600 g of washed and dried CIM in the form of iron fillings from a metal sawing machine (diameter 0.3–1.25 mm) was mixed with 12 L dry sand. The resulting CIM/sand ratio in this layer was thus 50 g·L⁻¹.

Filter 3 (ICS filter): On top of the 57 cm sand layer, a 25 cm layer composed of iron-coated sand (4 L) mixed with sand (8 L, same specifications as the intermediate layer). The iron-coated sand had a diameter range of 0.5–5 mm and average iron content of 40 g·L⁻¹ i.e., the total 160 g of iron was mixed into the specific media of Filter 3. The iron-coated sand was taken from a rapid sand-filtration (RSF) unit (Remon, type R700, Marum, The Netherlands) which is used in the lab for groundwater treatment.

2.3. Groundwater

All three filters were fed with groundwater pumped from a laboratory well and pre-treated by an RSF unit (Remon, type R700). Table 1 lists the physical–chemical characteristics of the pre-treated groundwater.

Table 1. Characteristics of the pre-treated groundwater used during the experiment compared with the health-based drinking water guidelines of the World Health Organization (WHO) [5].

Parameter	Measured Value	WHO Guideline for Drinking Water
Color	50 mg Pt-Co·L ⁻¹	No guideline, desirable: 15 mg Pt-Co·L ⁻¹
Turbidity	0.144 NTU	No guideline, desirable: <5 NTU
Conductivity	4.39 mS·cm ⁻¹	250 mS·cm ⁻¹
Redox potential	345 mV	No guideline
pH	7.31	No guideline, desirable: 6.5–8.5
Temperature	14.3 °C	No guideline
Dissolved oxygen	5.6 mg·L ⁻¹	No guideline
Sodium	461 mg·L ⁻¹	200 mg·L ⁻¹
Iron	0.09 mg·L ⁻¹	No guideline, desirable: 0.3 mg·L ⁻¹
Manganese	0.19 mg·L ⁻¹	0.5 mg·L ⁻¹
Ammonium	0.014 mg·L ⁻¹	No guideline
Nitrate	1.8 mg·L ⁻¹	50 mg·L ⁻¹
Phosphorus	0.25 mg·L ⁻¹	No guideline

To provide a specific concentration of arsenic in the influent, arsenic (III) oxide was spiked to the influent using a magnetic pump (see Figure 1). The flow rate was adjusted to provide a final concentration of ~70 µg·L⁻¹. The arsenic solution was pumped from a single reservoir and divided into the three filters. To provide better mixing, a mixing coil was used after the pump and before the filters.

2.4. Physical–Chemical Analyses

Samples of the influent (sampling point 01) and effluents (sampling point 02) for all the filters were collected twice per day (morning and afternoon), excluding the weekends, throughout the duration of the experiments. In the 4th, 12th and 27th experimental weeks, samples from sampling ports 03 to 07 were also taken in order to evaluate the arsenic-removal efficiency (and other parameters) along the filter(s) column. These samples were analysed for total arsenic concentration, total iron and manganese using inductively coupled plasma mass spectrometry (ICP-MS/iCap-Q/Thermo Scientific, Waltham, MA, USA). The same samples were also analysed regarding dissolved oxygen, pH, electrical conductivity and redox potential.

2.5. Microbiological Analyses

In experimental week 19, a sample was taken from the CIM filter top layer and analysed using real-time polymerase chain reaction (qPCR). The sample was analysed for the presence of four different micro-organisms, namely: (i) *Sphaerotilus* (groups 01 and 02); (ii) *Gallionella ferruginea*; (iii) *Leptothrix ochracea*; and (iv) *Leptothrix* sp. strain B2. These are micro-organisms that, according to the scientific literature, could potentially take part in biological arsenic removal [17]. The period of 19 weeks was given to allow the growth of such organisms in the filter(s) bio-layer.

2.6. Solid Vertical Profiles

At the end of the experiments, vertical profile samples of all the filters media were taken and analyzed regarding for the presence of different iron species with Raman spectroscopy. This analysis was conducted to verify possible chemical arsenic-removal mechanisms.

3. Results and Discussion

Figure 2a–c shows the arsenic concentration in the influents (diamonds) and effluents (squares) of the three filters throughout the duration of the experiment. From the figure it is possible to see a high fluctuation of the arsenic concentration in the influent during the first phase of the experiments (first 100 days). This was caused by hydraulic short circuits and malfunctioning of the first installed pump feeding arsenic to groundwater. Even though this phase provided a very unstable inlet arsenic concentration, the filters were kept in operation to verify the removal efficiency when arsenic is present in the influent at concentrations up to $200 \mu\text{g}\cdot\text{L}^{-1}$.

As can be seen in Figure 2b,d, the CIM filter was capable of keeping a good outlet arsenic concentration level, i.e., calculated median was $9.9 \mu\text{g}\cdot\text{L}^{-1}$. This was achieved also during the first phase of the experiments where influent arsenic concentration reached levels as high as $230 \mu\text{g}\cdot\text{L}^{-1}$. It is possible to see that, after 200 days of operation, the concentration level in the effluent of the same filter started to rise above $10 \mu\text{g}\cdot\text{L}^{-1}$. This was probably caused by depletion of the iron layer and/or saturation of the filter media. However, the concentration in the effluent was kept below the $50 \mu\text{g}\cdot\text{L}^{-1}$ limit (represented in the plots by dotted lines).

Figure 2c shows that the ICS filter also removed arsenic. However, the calculated median of the effluent arsenic concentration was $42 \mu\text{g}\cdot\text{L}^{-1}$.

The reference filter did not present any arsenic removal (Figure 2a,d).

Figure 3 summarizes the data obtained with the in-line measurements of electrical conductivity, pH and redox potential in the influent and effluents of the three filters. As can be seen, electrical conductivity and pH remained practically unchanged throughout the experimental time, whereas lower levels of redox potential were observed at the effluent of the CIM filter, possibly caused by oxidation of the CIM layer. These results will be further discussed when the Raman analysis results are presented.

Figure 4 shows the average results obtained when samples from sampling points 03 to 07 (see Figure 1) were taken and analyzed in terms of arsenic concentration. As can be seen, the average arsenic concentration in the CIM filter (red square symbols) is below $50 \mu\text{g}\cdot\text{L}^{-1}$ already in sampling port 03 and drops below $10 \mu\text{g}\cdot\text{L}^{-1}$ in sampling port 04, indicating that arsenic removal is indeed happening inside the CIM layer. In the ICS filter (green triangle symbols), arsenic concentration in sampling port 03 is also below $50 \mu\text{g}\cdot\text{L}^{-1}$; however, in sampling point 04 it remains well above $10 \mu\text{g}\cdot\text{L}^{-1}$.

The arsenic removal process in mixed media filters with iron takes place via oxidation of the iron matter, which leads to the formation of various iron oxides capable of sequestering arsenic from the liquid solution such as hydrous ferric oxides (HFO), lepidocrocite and goethite (see results of Raman spectroscopy further) [13]. As mentioned by Manning et al. [18], at $\text{pH} > 6.9$ and aerobic conditions ($\text{DO} > 1 \text{ mg}\cdot\text{L}^{-1}$), arsenite (As III) is oxidized into arsenate (As V). Both reactions, iron and arsenic oxidation, would contribute to oxygen consumption inside the filters which would decrease

the DO levels along the filtration column. This effect is clearly reflected in the results obtained with the monitoring of the DO levels along the filters' column.

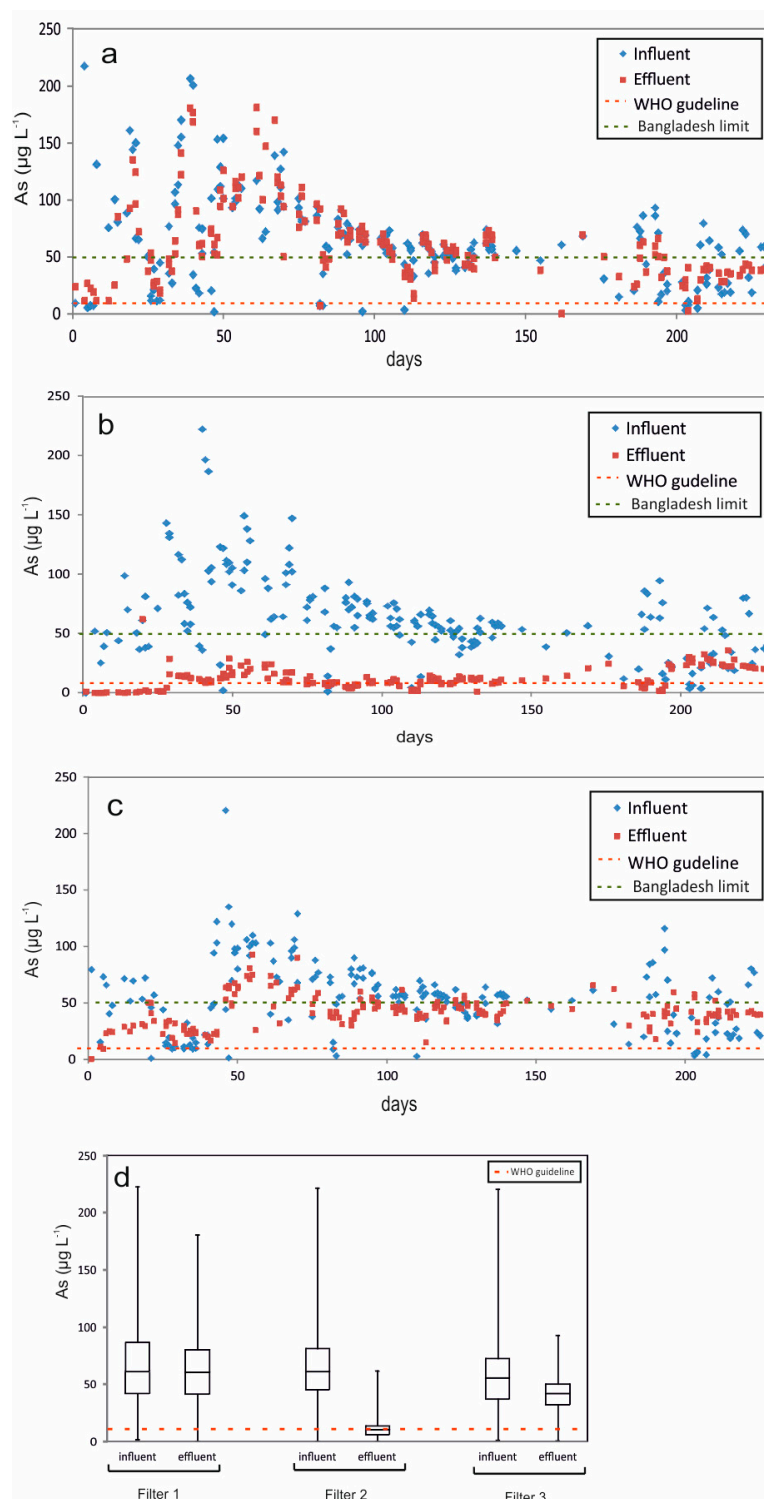


Figure 2. Arsenic removal by three different mixed-media slow-sand filters: concentrations measured throughout the experimental period in (a) reference filter, (b) CIM filter, (c) ICS filter and (d) boxplots summarizing results presented in plots (a–c).

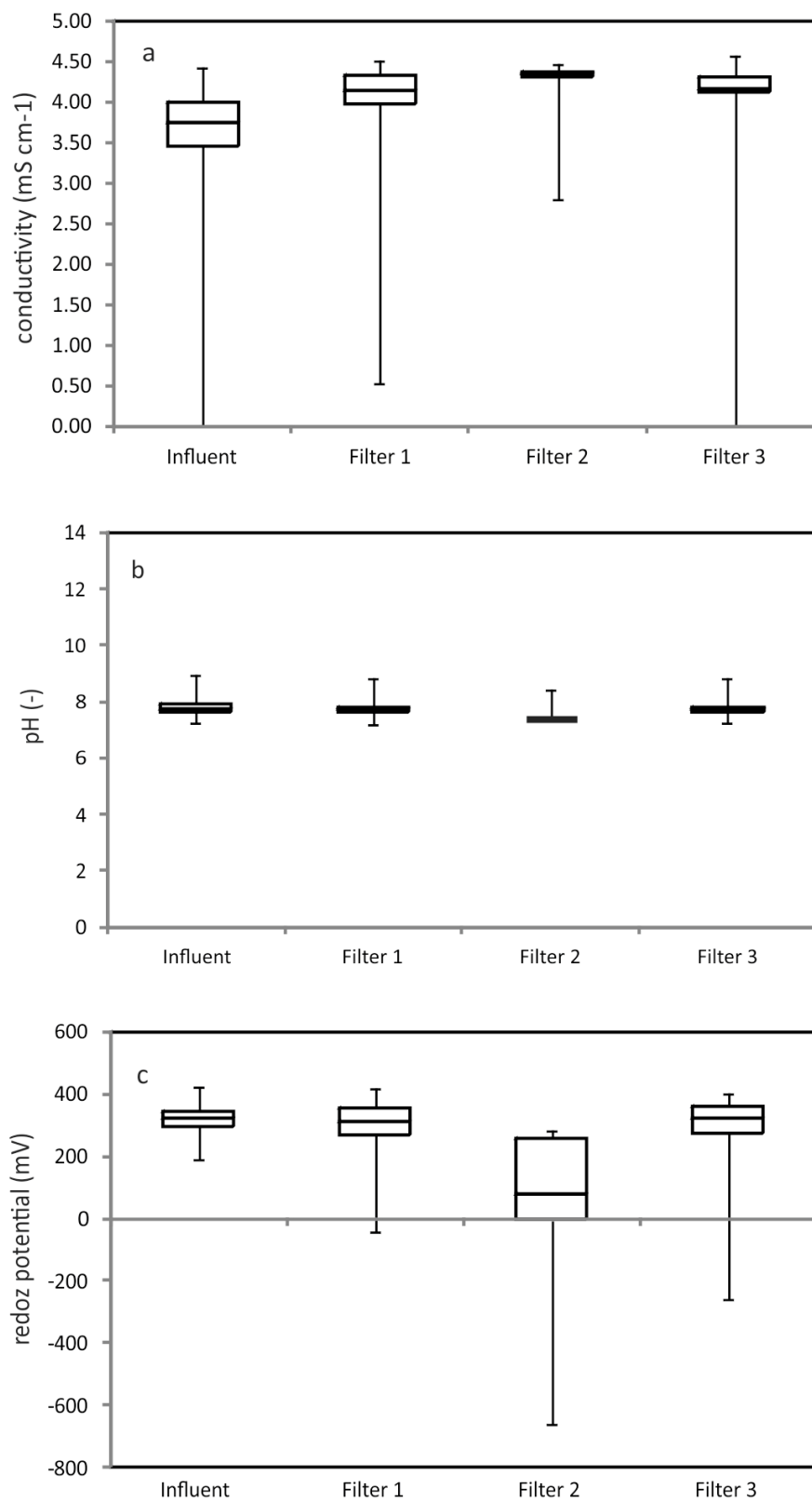


Figure 3. Boxplots representing the following physical–chemical parameters: (a) electrical conductivity, (b) pH, (c) redox potential, monitored inline in the influent and effluents of all three filters throughout the duration of the experiment.

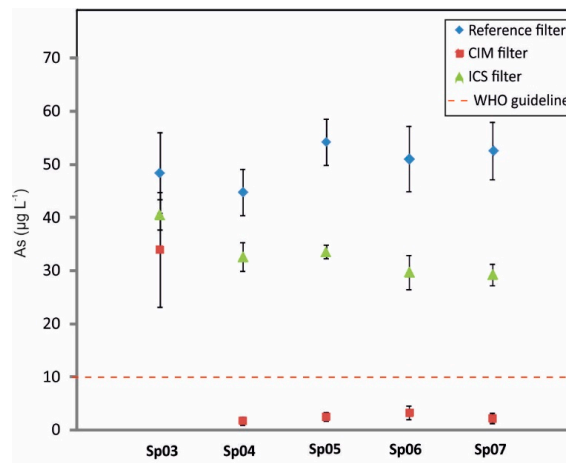


Figure 4. Arsenic concentration at different sampling ports (03 to 07) along the filter column.

Figure 5 shows a considerably lower level of DO after sampling port 3 for the CIM filter, while the other filters keep a stable DO level after the same port, i.e., indicating some biological activity of the top layer. The same trend was not reflected in the values of the redox potential measurement, most probably caused by the high oxidation potential of the influent.

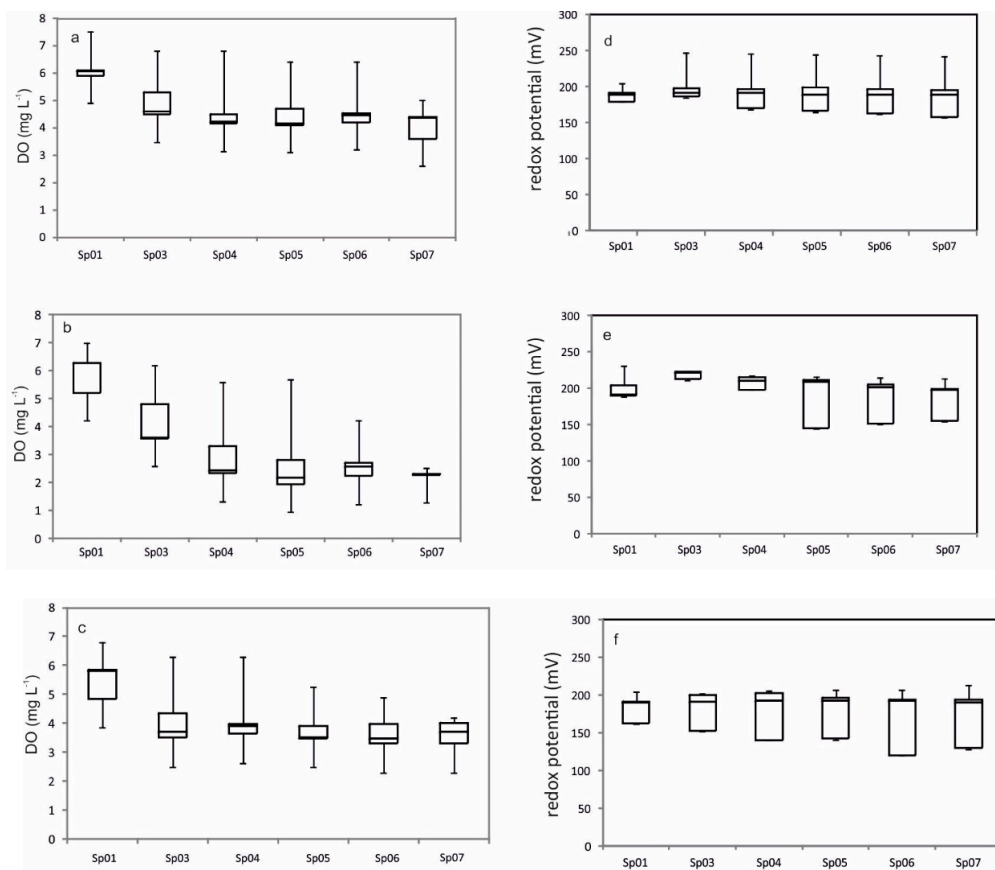


Figure 5. Box plot representation of the data obtained in the analysis of the vertical concentration profiles of dissolved oxygen (DO) and redox potential inside the three filters ((a,d)—reference filter; (b,e)—CIM filter; (c,f)—ICS filter).

Manganese and iron concentrations in the filters' influent and effluent were also investigated to verify possible competition with the oxidation of other metals (Mn) and/or metal leaching from the mixed-media layer (Fe). As shown in Figure 6b, while the influent concentration of aqueous iron is similar for all the filters, the effluent concentrations are comparably lower. This indicates iron consumption inside the filter and, consequently, that there is no iron leaching in the mixed-media filters. The evaluated populations presented, nevertheless, relatively high standard deviation and were, therefore, also compared using a hypothesis test ($\alpha = 0.05$, $H_0: \mu_{in} > \mu_{out}$ and $n = 100$). The results were positive (null hypotheses accepted) for all three filters. The results obtained suggest that Fe(0) was oxidized to Fe(III), which is much less mobile than Fe(II). This observation is in accordance with the Pourbaix diagram for iron, which indicates that in the conditions prevailing inside the filters, i.e., pH \sim 8 and positive redox potential, the immobile Fe(III) species will prevail.

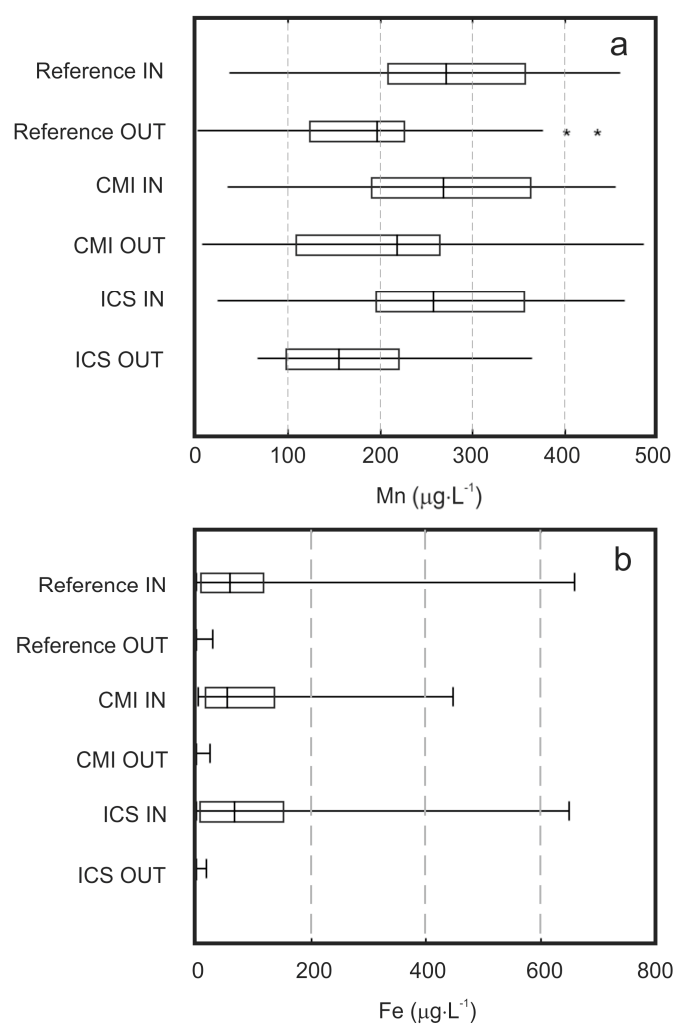


Figure 6. Box plot representation of the measured concentration of (a) manganese and (b) iron in the influents (IN) and effluents (OUT) of the three filters. Total (average) population for both samples was \sim 150 measured points. Outliers are represented by stars.

Figure 6a shows that manganese was not removed by the filters. This is to be expected, because the redox potential necessary for oxidation of this metal is much lower than for iron and arsenic. Therefore, oxygen is consumed first by the other two metals. If an efficient removal of manganese is also desirable, it can be achieved by the introduction of strong oxidants, e.g., chlorine. A hypothesis

test was also used to compare these data ($\alpha = 0.05$, $H_0: \mu_{in} = \mu_{out}$ and $n = 150$). The results obtained were also positive (null hypotheses accepted) for all three filters.

3.1. Corrosive Iron Matter (CIM) Composition

The Raman analysis of the original sand-filter material denoted three major bands at 118, 200 and 455 cm^{-1} , belonging to the out-of-plane Si-O vibrations [19]. These vibration bands are typical of quartz-like minerals and are used as the basis for the sand filters.

The analysis showed that the sample of the reference filter was composed of a dark top layer that extended for a few centimeters, while the majority of the sand kept its original form. It was not possible to characterize this material due to high fluorescence. The dark top layer was most probably organic material. The same problem was observed during the analysis of the samples from the ICS filter.

The samples from the CIM filter showed that a major part of the top layer was composed of zero-valent iron, Fe^0 . The influent was fed from the top such that it first interacted with the CIM layer. After several months of operation, the first 20 cm of the filter gained a reddish color. The color was gradually changing into yellow to the depth of 40 cm, beyond which the typical grey color of quartz predominated. Analysis with Raman spectroscopy on the first top layer showed similar bands of quartz and complementary bands that represented hydrous ferric oxide (HFO) (Figure 7). The 249 cm^{-1} and 380 cm^{-1} belong to the vibration bands of Fe-O, representing lepidocrocite ($\gamma\text{-FeOOH}$) [20,21]. The small band at 296 cm^{-1} and also 380 cm^{-1} are representative of goethite ($\alpha\text{-FeOOH}$) [17,18]. The 690 cm^{-1} probably represents HFO [21]. Minerals like magnetite (Fe_3O_4) were not observed or were present at low concentrations. Based on the peak size, the percentage of lepidocrocite was estimated to be about 80%, while that of ferrihydrite about 20%. The amount of goethite was small compared to these two phases and was, therefore, neglected.

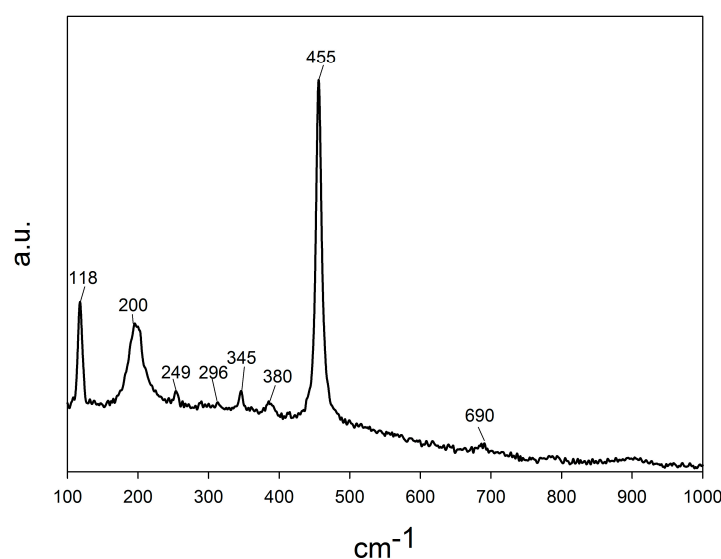


Figure 7. Raman spectra (100–1000 cm^{-1}) of first 40 cm of the CIM filter.

Finding a mixture of ferrihydrite, goethite and lepidocrocite in deeper parts of sand filters means that some of the top-placed Fe^0 was oxidized into Fe^{3+} ions and that these Fe^{3+} ions precipitated on the first 40 cm. It is unlikely that Fe^{3+} ions are those that migrated into deeper parts, as these ions have a very low solubility, i.e., 10^{-37} – 10^{-44} M^{20} , and with the influent pH of around 8, the concentration of Fe^{3+} ions would be around 10^{-19} – 10^{-26} M. The oxidation of $\text{Fe}^0 \rightarrow \text{Fe}^{3+} + 3\text{e}^-$, however, follows two steps: (1) $\text{Fe}^0 \rightarrow \text{Fe}^{2+} + 2\text{e}^-$ and (2) $\text{Fe}^{2+} \rightarrow \text{Fe}^{3+} + \text{e}^-$, where the intermediate Fe^{2+} ions have a solubility of 10^{-14} M [22]. The reason that lepidocrocite, goethite and HFO end up in deeper parts of the sand filter is likely due to migration of the more soluble Fe^{2+} ions followed by oxidation by O_2 and instant

precipitation on the parent sand filter. The decrease in DO from initial 5.1–7.0 mg·L⁻¹ (influent) to 2.3–2.5 mg·L⁻¹ (Figure 5) is an indication that DO was consumed for oxidizing the Fe²⁺-ions into Fe³⁺ ions. At the outlet, there were no Fe³⁺ ions measured, which means that all the Fe²⁺ ions generated were oxidized into Fe³⁺ ions and precipitated as lepidocrocite, goethite and/or HFO.

The analysis of the dissolved oxygen levels in the filters' columns provided a good quantitative indication of the oxidation of Fe²⁺ ions, i.e., to which extent the CIM mass is converted into lepidocrocite and HFO. As previously mentioned, the fact that this parameter also decreases in the reference filter indicates that oxygen is consumed by other processes (probably biological activity of the top layer) other than only the oxidation of Fe²⁺-ions. If it is assumed that the difference between the dissolved oxygen levels in the effluent of the reference filter and the CIM filter would realistically represent the amount of oxygen consumed by the oxidation of the CIM layer, one could determine approximately the oxidized CIM mass during the filter operation. Following this assumption, it was found that about 80% of the CIM mass was converted into lepidocrocite and HFO. If it is assumed that the total CIM mass (600 g) would be consumed, the iron consumption ratio in the CIM filter can be calculated as approximately 2 g·day⁻¹.

The active groups of lepidocrocite, goethite and HFO that bind the AsO₄³⁻ and AsO₃³⁻ ions are the ≡Fe-OH groups [23]. The binding of AsO₄³⁻ and AsO₃³⁻ ions to these oxides can be achieved in various ways, ranging from pure physical to monodentate or bidentate complex formation [24–26]. The ≡Fe-OH groups are typically amphoteric with pK_{a1} and pK_{a2} of ~6 and ~8 [23]. Assuming that the specific surface area of lepidocrocite and HFO are, respectively, 600 m²·g⁻¹ and 80 m²·g⁻¹, with typical site density of 4.2 OH·nm⁻² and 2.1 OH·nm⁻², the total active [≡Fe-OH] is around 1.9 mM [23]. Using Visual Minteq, a close approximation of the adsorption capacity with respect to AsO₄³⁻ and AsO₃³⁻ ions is about 5.8 mmol·g⁻¹ Fe, which is accompanied by 99.9% removal of As. This means that there was more than enough lepidocrocite and HFO formed to bind all the AsO₄³⁻—and AsO₃³⁻ ions. The 85% of As removal in the CIM filter (Figure 2) is in line with this. The fact that some fraction of the total As was not removed may be related to other competing ions binding to the surface of HFO and lepidocrocite, such as CO₃²⁻ [27,28] and PO₄³⁻ ions [29].

Two possible reasons can be presented for the low arsenic removal efficiency observed on the ICS filter. First, the total mass of iron in the ICS filter was relatively lower than in the CIM filter, i.e., 160 g as opposed to 600 g. Secondly, the iron-coated sand was obtained from a sand-filtration unit (Remon[®]) used for the pre-treatment of groundwater. This unit is built with nozzles on top of the sand media (shower system) to remove methane. The process is, thus, oxidizing the soluble iron present in the influent into HFO which can bind other organics (e.g., humic acids [29]), CO₃²⁻, [27,28] H₄SiO₄ [28] and PO₄³⁻ ions [29], compromising the binding with the AsO₄³⁻ and AsO₃³⁻ ions once introduced in the ICS filter. Such a process occurs less in the CIM filter, as the HFO and lepidocrocite are produced inside the media.

3.2. Biological Arsenic Removal

The top (biological) layer of the CIM filter was also investigated regarding the presence of four iron bacteria i.e., *Sphaerotilus*, *Gallionella ferruginea*, *Leptothrix ochracea* and strain B2 of *Leptothrix* sp. The results have only shown the presence of *Sphaerotilus* (see Table 2).

Table 2. Microbial investigation of the CIM filter top layer: detection limits and analysis results in number of cells per sample (N/sample, sample type: swab), based on the assumption that 1 DNA-copy is equal to 1 cell (n.d. = not detected).

Microorganism Type	Unit	Detection Limit	Analysis Results
<i>Sphaerotilus</i> (group 1 and group 2)	N/sample	4.0 × 10 ³	6.6 × 10 ³
<i>Gallionella ferruginea</i>	N/sample	4.0 × 10 ³	n.d.
<i>Leptothrix ochracea</i>	N/sample	4.0 × 10 ³	n.d.
<i>Leptothrix</i> sp. Strain B2	N/sample	4.0 × 10 ³	n.d.

According to the literature, some iron bacteria can precipitate iron present in groundwater and deposit it on their cell surface [17]. There, arsenic can be subsequently adsorbed and eventually removed from the aqueous phase. Even though the results showed the presence of iron bacteria, a biological arsenic-removal mechanism inside the filters is rather unlikely, mainly because, in that case, removal would also then be observed in the reference filter, i.e., all three filters presented a biological top layer. Among other aspects, the low iron concentration in the inlet was probably the limiting factor for biological arsenic removal in this case, i.e., according to the investigation by Pokhrel et al. [17,30], iron must be present in groundwater in concentrations at least 40 times higher than that of arsenic for biological arsenic-removal to be efficient. More detailed investigations would have to be conducted, however, including a more complete analysis of the microbiological population of the other two filters, in order to allow a better understanding of the influence of the biological activities of this type of filters on arsenic removal.

4. Conclusions

The results obtained in this work indicated that SSFs augmented with iron are a viable solution for the removal of arsenic from groundwater. The different mixed-media SSF systems investigated have, nevertheless, shown different results. First observations indicated a better performance of the filter with corrosive iron matter when compared to the iron-coated sand system. However, the latter showed some removal efficiency and it is believed that a better choice of iron-coated sand media would probably provide similar results as encountered for the other mixed-media system.

The results showed that the CIM filter, in the conditions of the experiment, presented an average arsenic concentration level of $9.9 \mu\text{g}\cdot\text{L}^{-1}$, i.e., below the maximum level indicated by the WHO. Additionally, throughout the whole duration of the experiments the filter only once provided effluent levels above the Bangladeshi limits of $50 \mu\text{g}\cdot\text{L}^{-1}$.

The analyses done to verify the As concentration levels along the filter column indicated that the removal is complete in the mixed-media layer. Additionally, dissolved-oxygen analysis, Raman spectroscopy analysis, and a short microbiological investigation analysis of the filter media indicated the removal mechanism is most probably predominantly chemical, even though iron bacteria were found to be present in the filter's top layer.

Raman spectroscopy analysis indicated that hydrous ferric oxides (HFO) and lepidocrochite were possibly the main iron oxide species responsible for the binding of arsenic in the CIM filter. Calculations based on the oxygen-consumption level of the CIM filters indicated that 80% of the CIM mass was consumed, which led to an approximate corrosive iron consumption ratio of $2 \text{ g}\cdot\text{day}^{-1}$.

Iron and manganese analysis of the filters' effluent indicated that no extra soluble iron species were present in the effluent of the mixed media filters and that manganese was not competing with iron for oxygen consumption and consequent arsenic removal.

Acknowledgments: The authors would like to acknowledge the financial support given by the Centre of Expertise Water Technology (CEW) for the realization of this work. Additionally, the participation of many students could only be made possible due to the financial support provided by the Science without Borders program financed by the Brazilian Federal Government, represented by CAPES.

Author Contributions: Luewton L. F. Agostinho and Leo Groendijk supervision and support during experiments design phase; Aize Tolsma, Timea Kolvac, Vlade Dalbosco lab work (setup maintenance and analysis); Kamuran Yasadi RAMAN analysis; Karolina M. Śmiech supervision and manuscript writing.

Conflicts of Interest: The authors declare no conflict of interest.

References

1. Chakraborti, D.; Rahman, M.M.; Das, B.; Murrill, M.; Dey, S.; Chandra Mukherjee, S.; Dhar, R.K.; Biswas, B.K.; Chowdhury, U.K.; Roy, S.; et al. Status of groundwater arsenic contamination in Bangladesh: A 14-year study report. *Water Res.* **2010**, *44*, 5789–5802. [[CrossRef](#)] [[PubMed](#)]

2. Chakraborti, D.; Rahman, M.M.; Mukherjee, A.; Alauddin, M.; Hassan, M.; Dutta, R.N.; Pati, S.; Mukherjee, S.C.; Roy, S.; Quamruzzman, Q.; et al. Groundwater arsenic contamination in Bangladesh—21 Years of research. *J. Trace Elem. Med. Biol.* **2015**, *31*, 237–248. [[CrossRef](#)] [[PubMed](#)]
3. Shakoor, M.B.; Niazi, N.K.; Bibi, I.; Rahman, M.M.; Naidu, R.; Dong, Z.; Shahid, M.; Arshad, M. Unravelling health risk and speciation of arsenic from groundwater in rural areas of Punjab, Pakistan. *Int. J. Environ. Res. Public Health* **2015**, *12*, 12371–12390. [[CrossRef](#)] [[PubMed](#)]
4. Shahid, M.; Khalid, M.; Dumat, C.; Khalid, S.; Niazi, N.K.; Imran, M.; Bibi, I.; Ahmad, I.; Hammad, H.M.; Tabassum, R.A. Arsenic level and risk assessment of groundwater in vehari, Punjab Province, Pakistan. *Expo. Health* **2017**. [[CrossRef](#)]
5. World Health Organization (WHO). *Guidelines for Drinking Water Quality*, 4th ed.; WHO Press: Geneva, Switzerland, 2011; ISBN 9789241548151.
6. Shakoor, M.B.; Niazi, N.K.; Bibi, I.; Murtaza, G.; Kunhikrishnan, A.; Seshadri, B.; Shahid, M.; Ali, S.; Bolan, N.S.; Ok, Y.S.; et al. Remediation of arsenic-contaminated water using agricultural wastes as biosorbents. *Crit. Rev. Environ. Sci. Technol.* **2016**, *46*, 467–499. [[CrossRef](#)]
7. Dhar, R.K.; Biswas, B.K.; Samanta, G.; Mandal, B.K.; Chakraborti, D.; Roy, S.; Jafar, A.; Islam, A.; Ara, G.; Kabir, S.; et al. Groundwater arsenic calamity in Bangladesh. *Curr. Sci.* **1997**, *73*, 48–59.
8. Smith, A.H.; Lingas, E.O.; Rahman, M. Contamination of drinking-water by arsenic in Bangladesh: A public health emergency. *Bull. World Health Organ.* **2000**, *78*, 1093–1103. [[PubMed](#)]
9. EPA-Washington, DC, US. *Office of Water. Technologies and Costs for Removal of Arsenic from Drinking Water*; US Environmental Protection Agency: Washington, DC, USA, 2000.
10. Ng, K.-S.; Ujang, Z.; Le-Clech, P. Arsenic removal technologies for drinking water treatment. *Rev. Environ. Sci. Biol.* **2004**, *3*, 43–53. [[CrossRef](#)]
11. Delowar, H.K.M.; Uddin, I.; Hassan, W.H.A.; Perveen, M.F.; Irshad, M.; Islam, A.F.M.S.; Yoshida, I. A comparative study of household groundwater arsenic removal technologies and their water quality parameters. *J. Appl. Sci.* **2006**, *6*, 2193–2200.
12. Sutter, A.; Hug, S. *Simple Filters for Arsenic Removal in Developing Countries*; ETH Zurich: Zürich, Switzerland, 2009.
13. Neumann, A.; Kaegi, R.; Voegelin, A.; Hussam, A.; Munir, A.K.M.; Hug, S.J. Arsenic removal with composite iron matrix filters in Bangladesh: A field and laboratory study. *Environ. Sci. Technol.* **2013**, *47*, 4544–4554. [[CrossRef](#)] [[PubMed](#)]
14. Ngai, T.K.K.; Murcott, S.; Shrestha, R.R.; Dangol, B.E.; Maharjan, M. Development and dissemination of KanchanTM Arsenic Filter in rural Nepal. *Water Supply* **2006**, *6*, 137–146. [[CrossRef](#)]
15. Tabbal, G. Technical and Social Evaluation of Three Arsenic Removal Technologies in Nepal. Master's Thesis, Massachusetts Institute of Technology, Cambridge, MA, USA, 2003.
16. Munir, A.K.M.; Rasul, S.B.; Habibuddowla, M.; Alauddin, M.; Hussam, A.; Khan, A.H. Evaluation of performance of Sono 3-kolshi filter for arsenic removal from groundwater using zero valent iron through laboratory and field studies. In Proceedings of the International Workshop on Technologies for Arsenic Removal From Drinking Water, Tokyo, Japan, 5–7 May 2001; pp. 171–189.
17. Pokhrel, D.; Viraraghavan, T. Biological filtration for removal of arsenic from drinking water. *J. Environ. Manag.* **2009**, *90*, 1956–1961. [[CrossRef](#)] [[PubMed](#)]
18. Manning, B.A.; Hunt, M.L.; Amrhein, C.; Yarmoff, J.A. Arsenic(III) and arsenic(V) reactions with zerovalent iron corrosion products. *Environ. Sci. Technol.* **2002**, *36*, 5455–5461. [[CrossRef](#)] [[PubMed](#)]
19. Kingma, K.J.; Hemley, R.J. Raman spectroscopic study of microcrystalline silica. *Am. Miner.* **1994**, *79*, 269–273.
20. De Faria, D.L.A.; Venancio Silva, S.; de Oliveira, M.T. Raman microspectroscopy of some iron oxides and oxyhydroxides. *J. Raman Spectrosc.* **1997**, *28*, 873–878. [[CrossRef](#)]
21. Larroumet, D.; Greenfield, D.; Akid, R.; Yarwood, J. Raman spectroscopic studies of the corrosion of model iron electrodes in sodium chloride solution. *J. Raman Spectrosc.* **2007**, *38*, 1577–1585. [[CrossRef](#)]
22. Schwertmann, U. Solubility and dissolution of iron oxides. *Plant Soil* **1991**, *130*, 1–25. [[CrossRef](#)]
23. Cornell, R.M.; Schwertmann, U. *The Iron Oxides, Structure, Properties, Reactions and Uses*, 2nd ed.; Wiley-VCH: Weinheim, Germany, 2003; pp. 221–236.
24. Jain, A.; Raven, K.P.; Loeppert, R.H. Arsenite and arsenate adsorption on ferrihydrite: Surface charge reduction and net OH⁻ release stoichiometry. *Environ. Sci. Technol.* **1999**, *13*, 1179–1184. [[CrossRef](#)]

25. Jessen, S.; Larsen, F.; Koch, C.B.; Arvin, E. Sorption and desorption of arsenic to ferrihydrite in a sand filter. *Environ. Sci. Technol.* **2005**, *39*, 8045–8051. [[CrossRef](#)] [[PubMed](#)]
26. Ona-Nguema, G.; Morin, G.; Juillot, F.; Calas, G.; Brown, G.E., Jr. EXAFS analysis of arsenite adsorption onto two-line ferrihydrite, hematite, goethite, and lepidocrocite. *Environ. Sci. Technol.* **2005**, *39*, 9147–9155. [[CrossRef](#)] [[PubMed](#)]
27. Appelo, A.J.; Van der Weijden, J.J.; Tournassat, C.; Charlet, L. Surface complexation of ferrous iron and carbonate on ferrihydrite and the mobilization of arsenic. *Environ. Sci. Technol.* **2002**, *36*, 3096–3103. [[CrossRef](#)] [[PubMed](#)]
28. Su, C.; Puls, R.W. Arsenate and arsenite removal by zerovalent iron: Silicate, carbonate, borate, sulfate, chromate, molybdate and nitrate relative to chloride. *Environ. Sci. Technol.* **2001**, *35*, 4562–4568. [[CrossRef](#)] [[PubMed](#)]
29. Jain, A.; Loeppert, R.H. Effect of competing anions on the adsorption of arsenite and arsenate by ferrihydrite. *J. Environ. Qual.* **1999**, *29*, 1179–1184. [[CrossRef](#)]
30. Lehimas, G.F.D.; Chapman, J.I.; Bourguine, F.P. Arsenic removal from groundwater in conjunction with biological-iron removal. *Water Environ. J.* **2001**, *15*, 190–192. [[CrossRef](#)]



© 2018 by the authors. Licensee MDPI, Basel, Switzerland. This article is an open access article distributed under the terms and conditions of the Creative Commons Attribution (CC BY) license (<http://creativecommons.org/licenses/by/4.0/>).